A germinal center–independent pathway generates unswitched memory B cells early in the primary response

Justin J. Taylor, Kathryn A. Pape, and Marc K. Jenkins

Department of Microbiology, Center for Immunology, University of Minnesota Medical School, Minneapolis, MN 55455

Memory B cells can be produced from the classical germinal center (GC) pathway or a less understood GC-independent route. We used antigen-based cell enrichment to assess the relative contributions of these pathways to the polyclonal memory B cell pool. We identified a CD38$^+$ GL7$^+$ B cell precursor population that differentiated directly into IgM$^+$ or isotype-switched (sw) Ig$^+$ memory B cells in a GC-independent fashion in response to strong CD40 stimulation. Alternatively, CD38$^+$ GL7$^+$ B cell precursors had the potential to become Bcl-6$^+$ GC cells that then generated primarily swIg$^+$ memory B cells. These results demonstrate that early IgM$^+$ and swIg$^+$ memory B cells are products of a GC-independent pathway, whereas later switched Ig$^+$ memory B cells are products of GC cells.

CORRESPONDENCE
Justin J. Taylor:
TAYL0611@umn.edu

Abbreviations used: AID, activation-induced cytidine deaminase; GC, germinal center.

Antibody-mediated immunity after primary infection or vaccination relies on the development and persistence of antigen-specific memory B cells and antibody-secreting plasma cells (MacLennan, 1994; McHeyzer-Williams and McHeyzer-Williams, 2005; Tarlinton, 2008; Maul and Gearhart, 2010). Plasma cells constitutively secrete antibody, which provides a first level of protection against infection with the original microbe. Plasma cells do not appear to respond to a second infection because of low surface expression of the membrane-bound version of Ig (BCR; Manz et al., 1998). Memory B cells, in contrast, maintain BCR expression and differentiate quickly into antibody-secreting cells after encountering the antigen a second time (Benson et al., 2009; Dogan et al., 2009; Pape et al., 2011).

Memory B cells are the progeny of rare naive B cells that express BCRs specific for the eliciting antigen. After antigen binding to the BCR and receipt of signals from helper T cells, naive B cells proliferate and undergo Ig isotype switching from IgM and IgD to IgG, IgA, or IgE (MacLennan, 1994; McHeyzer-Williams and McHeyzer-Williams, 2005; Tarlinton, 2008; Maul and Gearhart, 2010). The cells then differentiate into short-lived plasma cells that secrete antibodies, or germinal center (GC) cells, which then generate memory B cells and long-lived plasma cells (MacLennan, 1994; McHeyzer-Williams and McHeyzer-Williams, 2005; Tarlinton, 2008; Maul and Gearhart, 2010). Memory cells are selected in GC through a process involving acquisition of Ig somatic hypermutations that enhance antigen binding and allow successful competition for survival-promoting signals from helper T cells (MacLennan, 1994; McHeyzer-Williams and McHeyzer-Williams, 2005; Tarlinton, 2008; Maul and Gearhart, 2010).

Recent evidence, however, has posed challenges to this traditional model. First, several studies have noted the existence of memory B cells with IgM$^+$ BCRs (Klein et al., 1997, 1998; Anderson et al., 2007; Dogan et al., 2009; Pape et al., 2011). Moreover, these IgM$^+$ memory cells can outnumber the isotype-switched (swIg$^+$) memory cells of the same specificity (Dogan et al., 2009; Pape et al., 2011). Second, memory B cells and GC cells appear simultaneously (Blink et al., 2005; Chan et al., 2009), whereas the model predicts that GC cells should arise first. Lastly, not all memory B cells have Ig somatic mutations (Schittek and Rajewsky, 1992; Anderson et al., 2007; Pape et al., 2011) and memory B cells can be detected in mice that cannot form GC (Toyama et al., 2002). Collectively, the data indicate that Ig isotype switching, somatic mutation, and GC selection

The Rockefeller University Press $30.00
J. Exp. Med. Vol. 209 No. 3 597-606
www.jem.org/cgi/doi/10.1084/jem.20111696

The Journal of Experimental Medicine

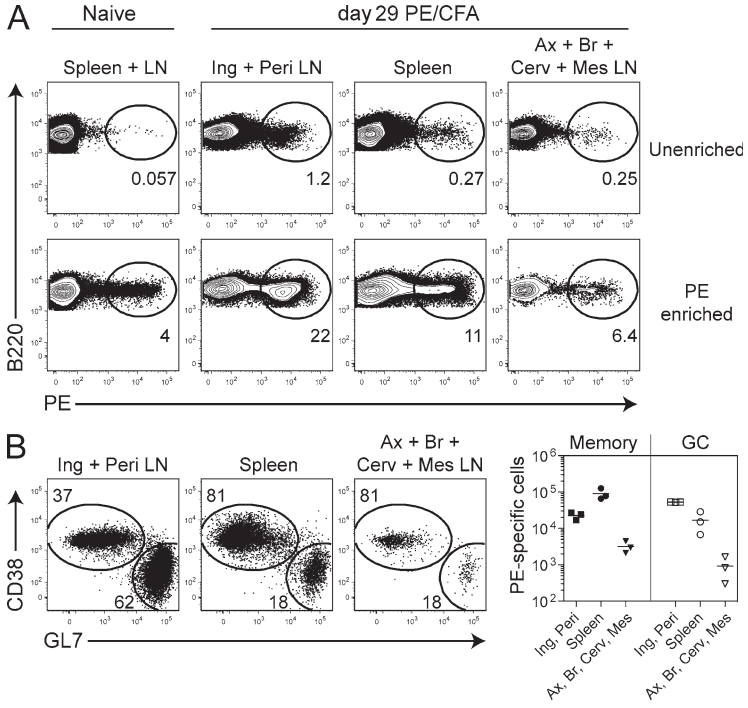

Figure 1. Early kinetics of the PE-specific B cell response. (A) Representative flow cytometry analysis of PE-specific B cells found in various lymphoid organs 29 d after s.c. injection of animals with 15 µg PE emulsified in CFA (PE/CFA) in the base of the tail and in the absence of injection. Each sample was analyzed directly ex vivo (top) or after ex vivo enrichment of PE-binding cells using anti-PE magnetic microbeads (bottom). The dots plots show B cells identified by flow cytometry in pooled spleen and LN samples as cells that stained with anti-B220 but not anti-Thy1.2, CD11c, Gr-1, or F4/80. Ing, inguinal LN; Peri LN, periaortic LN; Ax, axillary LN; Br, brachial LN; Cerv, cervical LN; Mes LN, mesenteric LN. Shown is a representative of two similar experiments. (B) Representative flow cytometry analysis of CD38 and GL7 expression by PE^+ B cells 29 d after injection of PE/CFA, along with the total number of donor PE-specific memory ($CD38^+$ $GL7^-$) and GC ($CD38^-$ $GL7^+$) B cells in the specified lymphoid organs. Each point represents an individual mouse and the bars represent the means ($n = 3$). Shown is a representative of two similar experiments.

are not required for memory cell generation. The GC-independent pathway of memory B cell formation, however, is not understood.

In this study, we assessed the contributions of the GC-dependent and -independent pathways of memory B cell formation using an antigen-based cell enrichment protocol that we recently developed (Pape et al., 2011). We focused on very early times in the primary response to identify the point at which the two pathways diverged. We found that GC-independent memory B cells were mainly $CD73^-$ and IgM^+ and were derived directly from a multipotent precursor that also produced GC cells. GC cells then generated mainly $swIg^+$ memory B cells, which could be identified by expression of CD73.

RESULTS

Detection and phenotypic analysis of antigen-specific B cells

Naive B cells specific for a given antigen are difficult to detect because they are rare among the 200×10^6 nucleated cells in the secondary lymphoid organs of a mouse. To analyze all antigen-specific B cells in these organs by flow cytometry, we developed a cell enrichment protocol that concentrates of the relevant cells into a sample containing $\sim 10^6$ cells (Pape et al., 2011). Using this method, we reported that 20,000 R-PE–specific and 4,000 allophycocyanin-specific B cells exist in the secondary lymphoid organs of individual C57BL/6 mice that had not been exposed to these antigens (Pape et al., 2011). In the same study, we tracked PE-specific memory and GC B cell formation from these naive precursors in the spleen and LN after s.c. immunization with PE emulsified in CFA.

Because the goal of the current study was to track GC-dependent and -independent memory cell formation, we examined various secondary lymphoid organs individually to get a better handle on the anatomy of the GC reaction in this system. As shown in Fig. 1 A, PE-specific naive B cells comprised a very small fraction of the total B cell population in an unenriched spleen and LN sample from an unimmunized B6 mouse. In contrast, the frequency of PE-specific B cells increased 21-fold over the starting frequency in the draining inguinal and periaortic LN 29 d after an s.c. injection of PE in CFA. The frequency of PE-specific B cells also increased in the spleen and nondraining LN, although only about fivefold. Enrichment with PE and anti-PE magnetic beads revealed a similar pattern of B cell clonal expansion while increasing the representation of PE-specific B cells in each sample. Analysis of the PE-specific B cells in the enriched samples showed that GC B cells ($GL7^+$) were more frequent in the PE-specific B cell population in the draining LN, although some GC B cells were present in other locations (Fig. 1 B). These results highlight the utility of the antigen-based cell enrichment method and support the approach of pooling the spleen and LN to capture the maximal number of GC-dependent B cells.

Early emergence of PE-specific memory B cells

A challenge for the early detection of memory B cells is the lack of a unique phenotypic marker that distinguishes these cells from naive B cells in mice. For example, both naive and memory B cells express the $CD38^+$ $GL7^-$ phenotype. Memory B cells, however, can be identified as $CD38^+$ $GL7^-$ B cells that divided in response to stimulation by antigen in the past. We tracked memory B cell formation using this criterion by transferring CFSE-labeled naive B cells from $CD45.1^+$ donor animals into congenic $CD45.2^+$ recipients. The gating used to detect $CD45.1^+$ PE^+ donor B cells is shown in Fig. 2 A. The great majority of PE-specific B cells remained $CFSE^{high}$ in unimmunized mice (Fig. 2 B) and proliferation was not induced after the injection of CFA alone (unpublished data). In contrast, $CD45.1^+$ donor PE-specific B cells began to proliferate

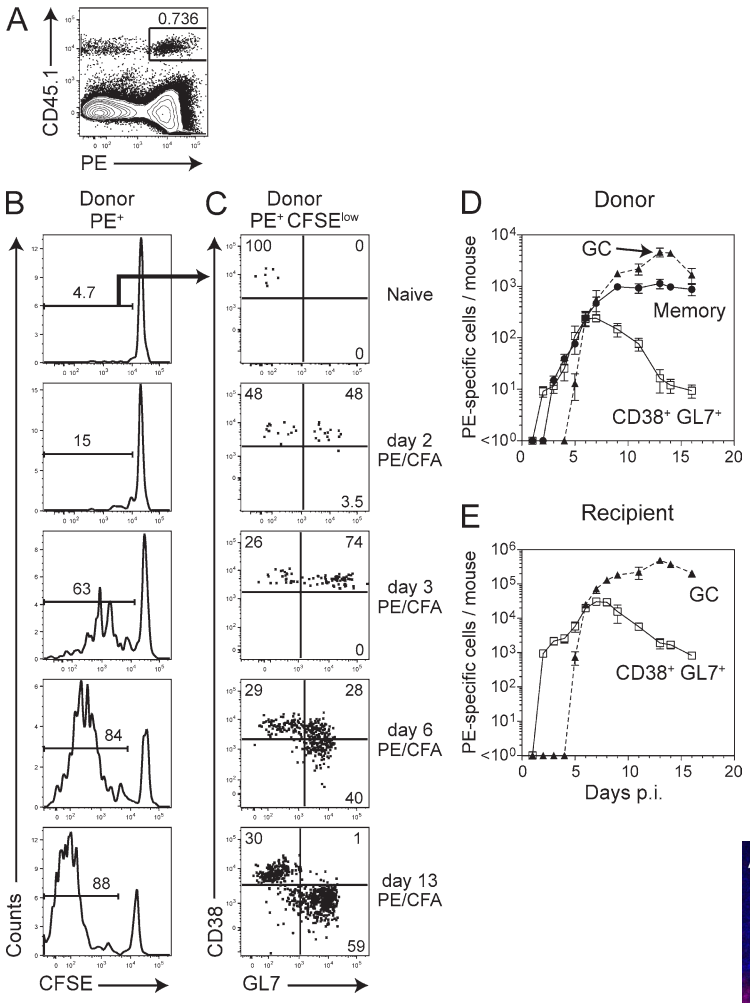

Figure 2. Early kinetics of the PE-specific B cell response. (A) Representative flow cytometry analysis showing the identification of donor CD45.1+ PE-specific B cells in the total B cell population (B220+, CD11c−, Gr-1−, and F4/80−) in a PE-enriched sample. (B) Representative flow cytometry analysis of CFSE dilution within donor PE-specific cells at the indicated time points after injection and without injection. p.i., post injection. (C) Representative flow cytometry analysis of CD38 and GL7 expression within CFSElow donor PE+ cells at the indicated time points after injection. (D) Combined data from 10 experiments showing the total number of donor PE-specific memory (CD38+ GL7−), GC (CD38− GL7+), and CD38+ GL7+ populations identified as shown in C, or using CellTrace violet instead of CFSE. The mean and SEM (n = 3–7) are shown for all time points. The mean number of cells in each population calculated in unimmunized mice (n = 8) was considered background and was subtracted from the displayed values. (E) Combined data from 10 experiments showing the total number of recipient (CD45.1−) PE-specific GC (CD38− GL7+) and CD38+ GL7+ cells. The mean and SEM (n = 3–14) are shown for all time points.

and lose CFSE between days 1 and 2 after injection of PE in CFA (Fig. 2 B) as observed in other immune responses (Chan et al., 2009; Coffey et al., 2009). Between days 2 and 4, the PE-specific CFSElow responding B cell population contained two subsets: CD38+ GL7− memory phenotype cells and CD38+ GL7+ cells (Fig. 2 C). The CD38+ GL7+ cells peaked at day 7 and declined rapidly thereafter (Fig. 2 D). CFSElow CD38+ GL7− memory B cells could be detected as early as day 3, with the majority of cells appearing between days 5 and 7 (Fig. 2 D). CD38− GL7+ GC B cells were not detected until day 5 but expanded robustly after that (Fig. 2 D). The absence of GC B cells before day 5 was not a limit of detection issue resulting from the adoptive transfer approach because similar kinetics were found when the total number of PE-specific GC B cells within the entire recipient animal was calculated (Fig. 2 E). Therefore, PE-specific CD38+ GL7+ B cells appeared at the same time as early CD38+ GL7− memory B cells and before CD38− GL7+ GC B cells.

Immunohistology was performed to further test the possibility that CD38+ GL7+ B cells form before GC B cells. As shown in Fig. 3 A, a few GL7− naive PE-specific B cells were detected at random locations in the follicles of mice that were not injected with PE. By day 4 after injection of PE in CFA, PE-specific B cells had increased in number. The majority of these cells (80%) were located at the T/B border, whereas most of the remaining cells were in the follicles (Fig. 3 B). About 30% of the PE-specific B cells expressed GL7 on day 4 and all of these cells

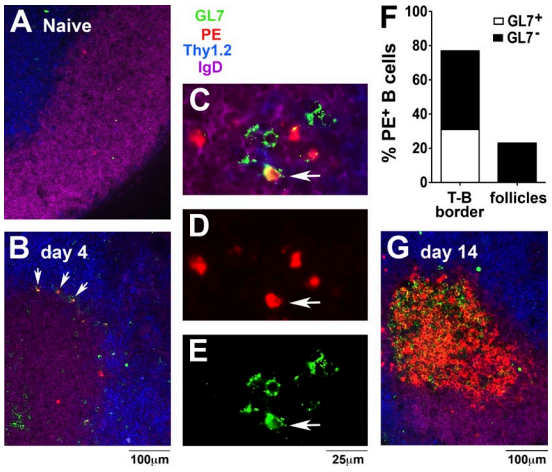

Figure 3. Co-localization of PE binding and GL7 staining B cells in situ. Sections of draining LN were stained with PE, followed by antibodies specific for GL7 (green), IgD (purple), Thy1.2 (blue), or PE (red). LN sections were from an unimmunized mouse (A) or from mice 4 d (B–E) or 14 d (G) after injection. Arrows in B show PE+ GL7+ cells (yellow) present at the T/B border. A close-up of a 4 d T/B border region shows the overlay of all colors (C), PE only (D), or GL7 only (E) with an arrow pointing to a double staining GL7+ PE+ cell. (F) The graph shows the percentage of the PE+ cells that were in the follicles or at the T/B border in sections of draining LN taken from PE/CFA-injected mice on day 4. The percentage of GL7+ PE+ cells is depicted with an empty bar and the percentage of GL7− PE+ cells is depicted with a filled bar. The T/B border was identified as a swath, 8–10 cells wide, where the IgD and Thy1.2 staining were mixed. The T cell areas, medullary chords, or any region not clearly resolved as follicle or T/B border were excluded from the analysis. 84 PE+ cells were counted in sections taken from 10 LNs obtained from five individual mice.

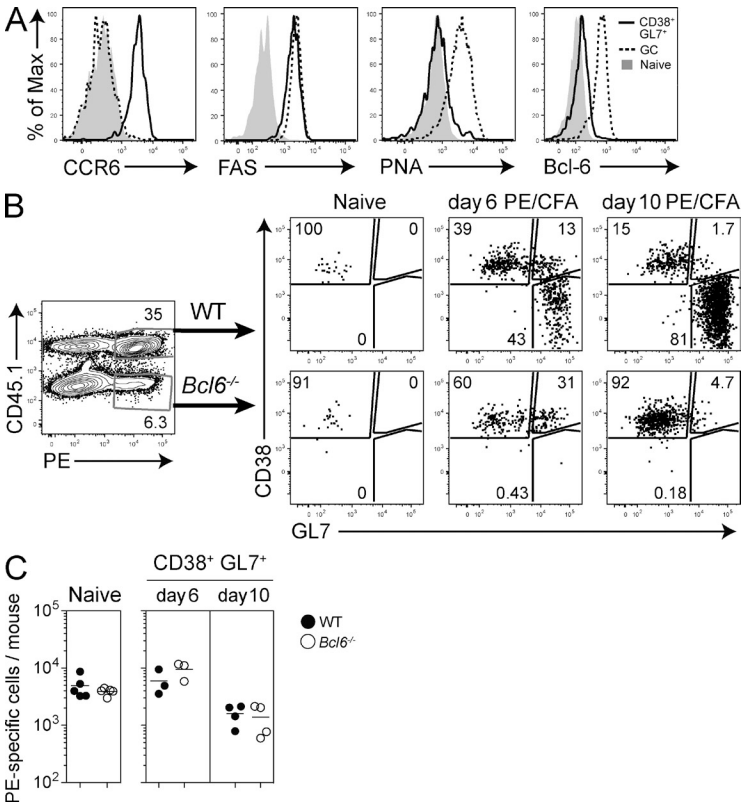

Figure 4. CD38⁺ GL7⁺ cells are distinct from GC cells. (A) Representative flow cytometry analysis of CCR6, FAS, PNA, and Bcl-6 expression on PE-specific naive (gray) or CD38⁺ GL7⁺ (solid line) or CD38⁻ GL7⁺ (dashed line) GC cells, 6 or 7 d after injection. Each marker was analyzed in at least three animals. (B) Representative flow cytometry analysis of CD38 and GL7 expression by PE-specific B cells in PE-enriched samples from mixed bone marrow chimeras containing CD45.1⁺ WT and *Bcl6*$^{-/-}$ cells at the noted times after injection. (C) Combined data from three experiments showing the total number of naive PE-specific WT and *Bcl6*$^{-/-}$ B cells in uninjected chimeras and CD38⁺ GL7⁺ B cells in chimeras injected with PE/CFA. Numbers are corrected for chimerism based on the ratio of WT and *Bcl6*$^{-/-}$ B cells that did not bind PE. The bars represent the means.

were located at the T/B border (Fig. 3, B–F). Nascent GCs were beginning to form at this time, but no PE-specific B cells were present in these structures (Fig. 3 B). In contrast, PE-specific B cells dominated the GCs at day 14 (Fig. 3 G). This in situ approach therefore confirmed the conclusion that CD38⁺ GL7⁺ B cells arise before GC B cells.

CD38⁺ GL7⁺ B cells are multipotent precursors

We sought to determine the relationship of the CD38⁺ GL7⁺ B cells to memory B cells and later GC B cells. A similar population of CD38⁺ B cells expressing the GC marker PNA has been hypothesized to be an early GC B cell (Shinall et al., 2000). In addition, Schwickert et al. (2011) found GL7⁺ CCR6⁺ FAS⁺ B cells at the border between the T cell areas and follicles of the draining LN and suggested that these were GC precursors. Similarly, we found that the PE-specific CD38⁺ GL7⁺ B cells induced by PE injection expressed CCR6 and FAS (Fig. 4 A). However, PE-specific CD38⁺ GL7⁺ B cells bound low levels of PNA compared with genuine CD38⁻ GL7⁺ GC B cells and did not express the GC fate-determining transcription factor Bcl-6 (Fig. 4 A). We tested the GC origin of CD38⁺ GL7⁺ B cells in radiation chimeras prepared with an equal mixture of *Bcl6*$^{-/-}$ and WT bone marrow cells. As reported by others (Dent et al., 1997; Fukuda et al., 1997; Toyama et al., 2002; Nurieva et al., 2009), Bcl-6 was required for the formation of CD38⁻ GL7⁺ GC B cells (Fig. 3 B). In contrast, CD38⁺ GL7⁺ B cells formed equally well from *Bcl6*$^{-/-}$ and WT precursors (Fig. 4 C). Therefore, the PE-specific CD38⁺ GL7⁺ B cells did not appear to be committed to the GC pathway.

The early appearance of CD38⁺ GL7⁺ B cells after PE immunization raised the possibility that they were precursors of early memory cells and GC cells. To test this hypothesis, CD38⁺ GL7⁺ B cells from animals injected with PE in CFA 4 d previously were purified and transferred into recipient animals injected with PE in CFA at the same time as the donors (Fig. 5 A). CD38⁺ GL7⁻ memory B cells emerged from CD38⁺ GL7⁺ donor B cells as early as day 2 after transfer (Fig. 5, B and C). GC B cells were also generated from the CD38⁺ GL7⁺ donor population, but not until day 4 after transfer (Fig. 5, B and C). Notably, CD38⁺ GL7⁺ B cells transferred into uninjected or CFA-injected recipients differentiated exclusively into memory B cells within 2 d after transfer (Fig. 5, B and C). Thus, CD38⁺ GL7⁺ B cells produced GC and memory B cells early in the primary response but only produced memory B cells when removed from antigen.

Quantifying GC-derived and -independent memory B cells

The results pointed to two pathways of memory cell formation. In one pathway, CD38⁺ GL7⁺ B cells differentiated directly into early memory cells without a GC cell intermediate. In the other, CD38⁺ GL7⁺ B cells differentiated into GC cells, some of which then became memory cells. We next aimed to determine the number of memory B cells that were generated from each pathway. This was done by counting memory B cells produced from WT or *Bcl6*$^{-/-}$ naive cells in the mixed chimeras described in Fig. 4. Because Bcl-6 is required for GC cell formation, any memory B cells that arise from *Bcl6*$^{-/-}$ naive B cells must be derived from the GC-independent pathway. IgM⁺ and swIg⁺ memory B cells were also identified in these experiments.

The number of IgM⁺ memory B cells generated by *Bcl6*$^{-/-}$ cells was comparable to the number generated from WT cells at all time points analyzed (Fig. 6, A and B). In contrast, the number of *Bcl6*$^{-/-}$ swIg⁺ memory B cells was similar to WT at day 6, but reduced threefold at day 10 and 30-fold at day 30 (Fig. 6 C). Thus, IgM⁺ and early swIg⁺ memory B cells were generated in a GC-independent fashion, presumably directly from CD38⁺ GL7⁺ precursors, whereas >95% of later swIg⁺ memory B cells were GC derived.

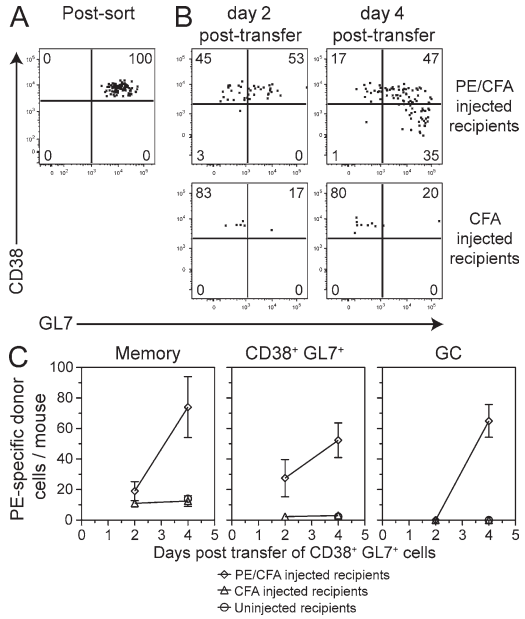

Figure 5. CD38$^+$ GL7$^+$ cells directly give rise to memory cells and GC cells. 4 d after injection with PE/CFA, total GL7$^+$ cells from CD45.1$^+$ animals were FACS purified and adoptively transferred into CD45.2$^+$ recipients. (A) Representative flow cytometry plots showing the expression of CD38 and GL7 on PE-specific B cells at the time of adoptive transfer. (B) Representative flow cytometry analysis of CD38 and GL7 expression by the donor CD45.1$^+$ PE-specific B cells 2 or 4 d after adoptive transfer into mice injected with PE and CFA or CFA alone at the same time as the donor animals. Data from two individual animals was concatenated for display. (C) Combined data from four experiments showing the total number of PE$^+$ donor memory (CD38$^+$ GL7$^-$), GC (CD38$^-$ GL7$^+$), and CD38$^+$ GL7$^+$ cells 2 and 4 d after transfer into uninjected mice or those injected with PE/CFA or CFA alone. The mean and SEM (n = 3–7) are shown.

One potential caveat to these experiments was that cells that would have differentiated into GC cells were artificially shunted into the memory cell compartment when unable to express Bcl-6. We therefore aimed to distinguish GC-derived memory B cells from GC-independent memory B cells in WT animals. This was accomplished by using CD73 (ecto-5′-nucleotidase) expression to mark GC-derived memory B cells. CD73 is expressed by subsets of IgM$^+$ and swIg$^+$ memory B cells that have high levels of somatic hypermutation (Anderson et al., 2007; Tomayko et al., 2010) and expressed activation-induced cytidine deaminase (AID; Dogan et al., 2009), a molecule required for somatic hypermutation and Ig isotype switching. Given that somatic mutations are thought to occur predominantly in GC B cells, CD73 was a good candidate to mark GC-derived but not GC-independent memory B cells. This possibility was tested by analysis of WT plus *Bcl6*$^{-/-}$ mixed chimeras. *Bcl6*$^{-/-}$ B cells that were incapable of forming GC cells generated the same number of CD73$^-$ IgM$^+$ memory B cells 31 d after immunization and only twofold less CD73$^-$ swIg$^+$ memory cells than WT B cells (Fig. 7, A and B). In contrast, *Bcl6*$^{-/-}$ B cells produced fivefold fewer CD73$^+$ IgM$^+$ memory B cells and 100-fold fewer CD73$^+$ swIg$^+$ memory B cells (Fig. 7, A and B) than WT B cells at this time. Similarly, CD40 ligand blockade beginning at day 5 (Fig. 7 C) or day 17 (unpublished data), which reduced the number of GC B cells by 95% (Han et al., 1995; unpublished data), also resulted in a significant decrease in the number of CD73$^+$ memory B cells present on day 30. Collectively, the data indicate that most GC-derived memory B cells express CD73, whereas most GC-independent memory B cells do not.

This conclusion was further supported by the kinetics of CD73$^-$ and CD73$^+$ memory B cell formation in WT mice. As shown in Fig. 8 A, the number of PE-specific GC B cells peaked 14 d after injection of PE and CFA. Consistent with GC-independent differentiation, the vast majority of IgM$^+$ memory B cells present at any time were CD73$^-$, as were the swIg$^+$ memory B cells that formed before the GC peak (Fig. 8, B and C). Consistent with GC-dependent differentiation, most swIg$^+$ memory B cells present after the GC peak were CD73$^+$ (Fig. 8 C). Furthermore, swIg$^+$ CD73$^-$ memory B cells declined dramatically after day 10 (Fig. 8 D) in the same way

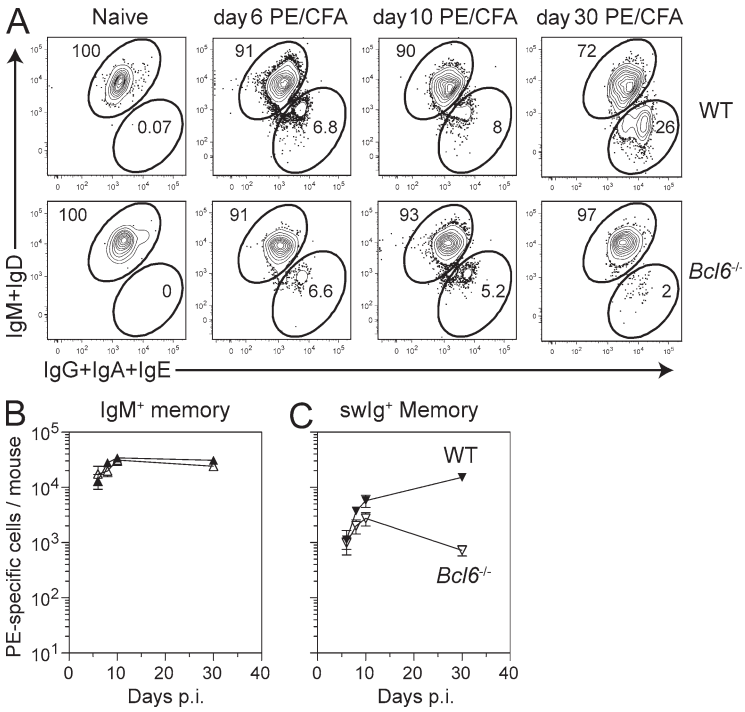

Figure 6. Quantifying GC-derived and GC-independent memory B cells. (A) Representative flow cytometry plots showing the expression of isotype switched (IgG$^+$IgA$^+$IgE$^+$) and unswitched (IgM$^+$IgD$^+$) Ig on PE-specific WT and *Bcl6*$^{-/-}$ memory populations (CD38$^+$ GL7$^-$) in WT:*Bcl6*$^{-/-}$ mixed chimeras at the indicated time points after injection. p.i., post injection. Combined data from five experiments showing the numbers of PE-specific WT and *Bcl6*$^{-/-}$ (B) IgM$^+$ memory and swIg$^+$ (C) memory cells. The mean and SEM (n = 3–5) are shown for all time points.

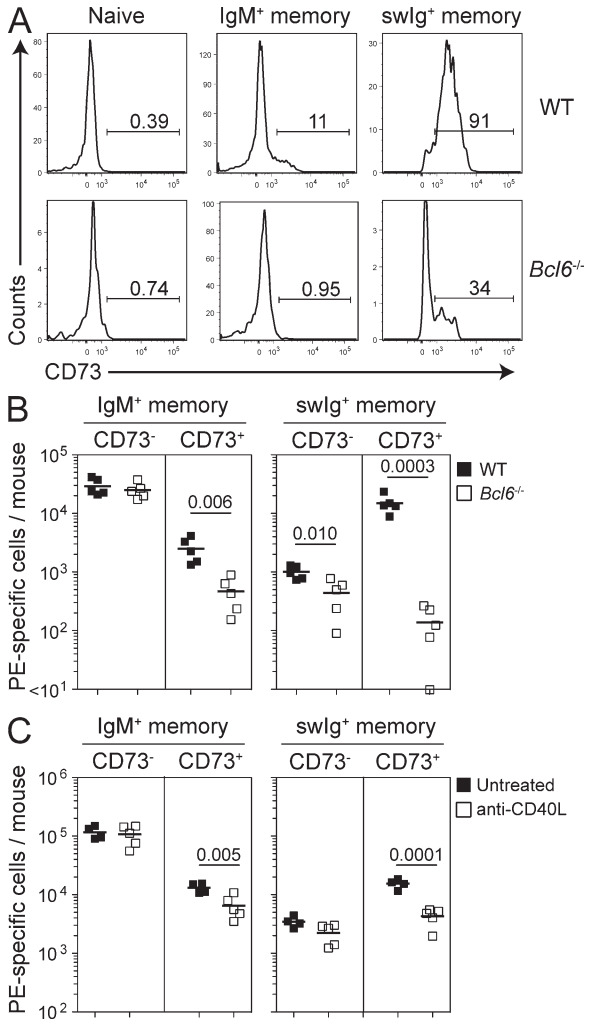

Figure 7. CD73 expression identifies most GC-derived memory B cells. (A) Representative flow cytometry plots from WT:*Bcl6*$^{-/-}$ mixed chimeras showing the expression of CD73 on PE-specific WT and *Bcl6*$^{-/-}$ IgM$^+$ and swIg$^+$ memory populations 30 d after injection, and the naive PE-specific cells found in uninjected mice. (B) Combined data from two experiments showing the numbers of PE-specific WT and *Bcl6*$^{-/-}$ CD73$^-$ and CD73$^+$ memory populations 31 d after injection. (C) Numbers of PE-specific CD73$^-$ and CD73$^+$ memory populations 31 d after injection, treated with or without anti-CD40L beginning on day 5. The bars in B and C indicate the means. P-values are shown for the indicated comparisons.

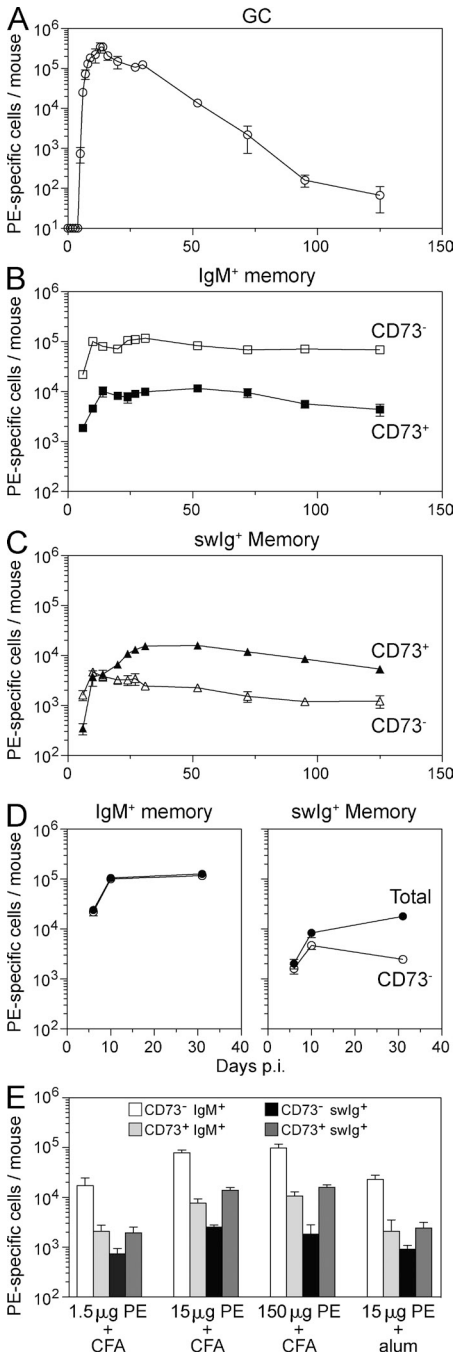

Figure 8. Quantifying CD73$^-$ and CD73$^+$ memory B cells. Combined data from five experiments showing the numbers of PE-specific (A) GC cells, IgM$^+$ CD73$^-$ and CD73$^+$ memory cells (B), or swIg$^+$ CD73$^-$ and CD73$^+$ memory cells (C) at the indicated time points after injection. (D) Combined data from multiple experiments showing the numbers of CD73$^-$ and total (CD73$^-$ + CD73$^+$) PE-specific memory cells and at days 6, 10, and 30. The mean and SEM (n = 3–6) are shown for A–D. (E) Combined data from two experiments showing the numbers of IgM$^+$ CD73$^-$, IgM$^+$ CD73$^+$, swIg$^+$ CD73$^-$, and swIg$^+$ CD73$^+$ memory cells 60 d after injection with 1.5, 15, or 150 µg PE in CFA or 15 µg PE adsorbed to alum. To account for unstimulated naive cells contaminating the IgM$^+$ CD73$^-$ population, the mean number of PE-specific cells found in unimmunized animals was subtracted from the IgM$^+$ CD73$^-$ population. The means and SEM (n = 3–6) are shown.

that GC-independent swIg$^+$ *Bcl6*$^{-/-}$ memory B cells declined (Fig. 6). These results confirm the conclusion that IgM$^+$ and early swIg$^+$ memory B cells are generated in a GC-independent fashion, whereas most later swIg$^+$ memory B cells are GC derived.

It was possible that the abundance of GC-independent CD73$^-$ IgM$^+$ memory B cells was unique to priming with 15 µg PE in CFA. However, a 10-fold increase in the dose of injected PE to 150 µg induced the same number of CD73$^+$ and CD73$^-$ memory B cells as injection of 15 µg (Fig. 8 E). A 10-fold reduction in the dose of injected PE to 1.5 µg resulted in a fivefold decrease in the total number of memory B cells,

but the relative frequency of the CD73$^+$ and CD73$^-$ subsets was largely unaffected (Fig. 8 E). Likewise, the use of alum as an adjuvant resulted in a decrease in the total number of memory B cells, but the relative frequencies of the CD73$^+$ and CD73$^-$ subsets were similar to those induced by CFA (Fig. 8 E). These results indicate that large numbers of GC-independent IgM$^+$ memory B cells are generated across a broad range of antigen doses and with two different adjuvants.

BCR and CD40 stimulation are sufficient for GC-independent memory cell formation

Earlier work demonstrated that CD40 signaling was required for antigen-driven B cell expansion and GC formation but, paradoxically, strong CD40 signaling with an agonistic CD40 antibody suppressed GC formation (Erickson et al., 2002). We used this antibody to test the possibility that T cell–derived CD40 signals were involved in the formation of GC-independent memory B cells. Consistent with prior work (Erickson et al., 2002), we found that administration of anti-CD40 at the time of injection of PE in CFA inhibited the formation of PE-specific GC B cells while slightly enhancing the formation of CD38$^+$ GL7$^+$ precursors and IgM$^+$ and swIg$^+$ memory B cells in WT mice (Fig. 9 A). The capacity of anti-CD40 to influence memory B cell formation was then tested in *Tcra*$^{-/-}$ T cell–deficient mice to determine if strong CD40 signaling was sufficient for the generation of GC-independent memory B cells. As reported previously (Pape et al., 2011), none of the activated phenotypes of PE-specific B cells were generated in *Tcra*$^{-/-}$ T cell–deficient mice injected with PE in CFA (Fig. 9 A). In contrast, PE-specific CD38$^+$ GL7$^+$ precursors and later IgM$^+$ and swIg$^+$ memory B cells were generated at or above WT levels in T cell–deficient mice injected with PE in CFA and anti-CD40, whereas GC B cells did not form at all (Fig. 9 A). Notably, the PE-specific swIg$^+$ memory B cells found in anti-CD40–treated animals were CD73$^-$ (Fig. 9 B), providing additional evidence that they were derived from the GC-independent pathway. Thus, strong CD40 stimulation is required for CD38$^+$ GL7$^+$ B cell generation and sufficient for GC-independent memory B cell differentiation.

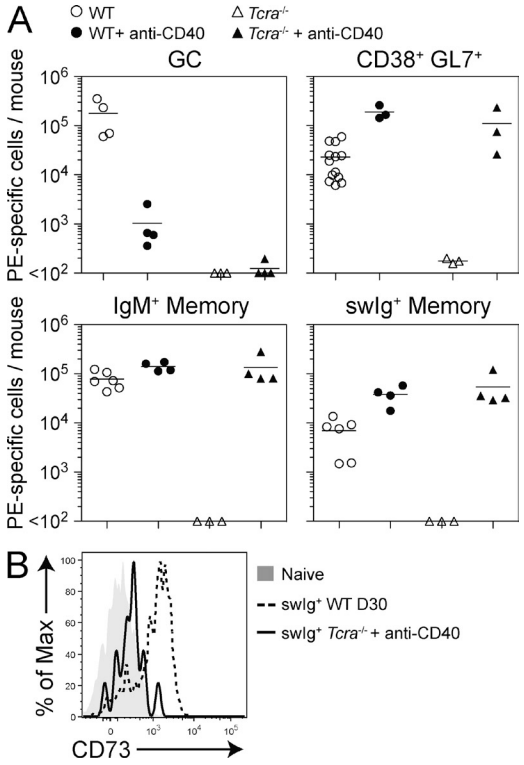

Figure 9. Agonistic CD40 stimulation induces GC-independent memory cell generation in the absence of T cells. (A) Combined data from three experiments showing the numbers of PE-specific GC, CD38$^+$ GL7$^+$ cells, IgM$^+$ memory, and swIg$^+$ memory cells in WT and *Tcra*$^{-/-}$ mice with or without treatment with 250 µg anti-CD40 every other day beginning at the time of PE/CFA injection. The numbers of CD38$^+$ GL7$^+$ cells were calculated 6 d after injection, whereas the other populations were assessed at 9 d. To account for unstimulated naive cells contaminating the IgM$^+$ memory population, the mean number of PE-specific cells found in uninjected animals was subtracted from the IgM$^+$ population. Each data point represents an individual mouse and bars represent the mean. (B) Representative flow cytometry plots showing the expression of CD73 on PE-specific naive cells or swIg$^+$ memory cells found in anti-CD40–treated *Tcra*$^{-/-}$ mice 9 d after injection or WT mice 30 d after injection. Shown is a representative of three animals.

DISCUSSION

Our results show that GC-independent and GC-dependent memory B cells arise from developmentally plastic CD38$^+$ GL7$^+$ precursors. These precursors were capable of differentiating directly into memory B cells, mainly of the IgM$^+$ variety, without passing through a GC cell intermediate stage. Alternatively, these precursors were capable of differentiating into GC B cells, some of which then became memory B cells, mainly of the swIg$^+$ type. Therefore, our work confirmed earlier studies reporting that CD38$^+$ GL7$^+$ B cells could produce genuine GC B cells, but extended that work by showing that CD38$^+$ GL7$^+$ B cells could also directly generate GC-independent memory B cells.

Our results and the literature suggest the following scenario for the formation of CD38$^+$ GL7$^+$ B cells and their progeny. Previous work showed that naive B cells migrate to the border between the T and B cell areas after antigen binding and present antigen-derived peptide–MHCII complexes to helper T cells (Garside et al., 1998). This interaction results in CD40 signaling in the B cells causing them to proliferate (Garside et al., 1998). Our present work and that of Schwickert et al. (2011) suggests that CD38$^+$ GL7$^+$ B cells are early progeny of this proliferation at the T/B border. Our results further suggest that strong CD40 signals can cause CD38$^+$ GL7$^+$ B cells to differentiate directly into memory B cells without passing through a GC stage. Like Erickson et al. (2002), we observed that agonistic anti-CD40 treatment suppresses GC B cell formation in WT mice where T cell help is present. This suggests that strong CD40 signaling favors early memory cell formation by inhibiting GC B cell formation in a dominant fashion. Together, these results suggest that BCR and CD40 signals

are required to generate CD38$^+$ GL7$^+$ B cells and that strong CD40 signaling directs these cells to become GC-independent memory B cells by preventing differentiation into GC B cells. Under normal circumstances, the B cells that receive these strong CD40 signals and become GC-independent memory B cells may be those that display large numbers of antigen-derived peptide–MHCII complexes, which induce large amounts of CD40 ligand on cognate helper T cells. In this model, CD38$^+$ GL7$^+$ B cells that receive weaker CD40 signals by interacting with a helper T cell displaying less CD40 ligand and providing other signals, such as IL-21, may differentiate into GC B cells.

CD38$^+$ GL7$^+$ B cells also converted into memory B cells when transferred into unimmunized mice. It is possible that some CD38$^+$ GL7$^+$ B cells received a strong CD40 signal and committed to the memory cell fate at the time of transfer, and simply completed this program in the antigen-free host. Alternatively, removal of BCR and CD40 stimulation may be a second pathway by which CD38$^+$ GL7$^+$ B cells become memory cells.

Validation of CD73 as a marker of GC-derived memory B cells allowed us to show that these memory cells arise 6 d after injection and are mostly swIg$^+$. The abundance of swIg$^+$ cells in the GC-dependent memory B cell population was expected because GC B cells express large amounts of AID. Accordingly, these memory cells have more somatic mutations and have undergone more affinity maturation than IgM$^+$ memory cells (Pape et al., 2011). Blink et al. (2005) found that the frequency of IgG1$^+$ memory B cells in the blood was similar at early and late times after immunization, whereas the fraction of the cells in the population with somatic hypermutations increased. This finding suggested that the IgG1$^+$ memory cells found early in the response were short-lived and replaced by IgG1$^+$ memory B cells coming from the GC at later time points. Although this is likely the case, the consistent decline of swIg$^+$ memory B cells over long periods of time observed in our experiments (Pape et al., 2011) indicates that even the GC-selected swIg$^+$ memory B cells have shorter half-lives than IgM$^+$ memory B cells.

The result that most IgM$^+$ memory B cells are GC independent explains our previous data showing that these cells exhibit a low level of somatic hypermutation (Pape et al., 2011). This result suggests that these cells did not express optimal amounts of AID, which is required for Ig isotype switching and somatic hypermutation. However, a population of IgM$^+$ memory B cells containing BCR somatic mutations was marked in an AID reporter mouse described by Dogan et al. (2009). These IgM$^+$ memory cells expressed CD73 (Dogan et al., 2009) and are likely the counterparts of the small GC-derived population of PE-specific CD73$^+$ IgM$^+$ memory B cells observed here.

In contrast, the data in humans indicates that most IgM$^+$ memory B cells are GC derived (Klein et al., 1998; Seifert and Küppers, 2009). The difference between these conclusions may be the result from the use of CD27 to define memory B cells in humans. This definition may exclude GC-independent memory B cells because CD27 was adopted as a memory cell marker based on the fact that both CD27$^+$ swIg$^+$ and CD27$^+$ IgM$^+$ contained high levels of somatic hypermutation, whereas CD27$^-$ IgM$^+$ cells lack mutations (Klein et al., 1998; Seifert and Küppers, 2009). Because nearly all individual CD27$^+$ IgM$^+$ B cells contain somatic mutations (Klein et al., 1998) and show other signs of passage through GC (Seifert and Küppers, 2009), it seems likely that GC-independent memory B cells reside within the CD27$^-$ IgM$^+$ fraction. Consistent with this notion, ∼25% of swIg$^+$ cells in human blood do not express CD27, are present, and show low levels of somatic hypermutation (Fecteau et al., 2006). Thus, the CD27$^-$ population of human B cells likely contains the products of this GC-independent pathway. CD27, which is up-regulated by GC B cells themselves (Jung et al., 2000), may simply be maintained by memory B cells after they leave the GC, whereas cells that bypass the GC never receive the stimulus to up-regulate CD27. In this way, CD27 expression in humans may be equivalent to CD73 expression in the mouse.

MATERIALS AND METHODS

Animals. 6–10-wk-old sex-matched mice were used for experiments. C57BL/6 (B6), *Tcra*$^{-/-}$, B6.CD45.1 congenic (B6.SJL-*Ptprc*^{a} *Pep3*^{b}/BoyJ), and 129Sv mice were purchased from The National Cancer Institute or The Jackson Laboratory and bred in house. *Bcl6*$^{-/-}$ mice on a mixed C57BL/6-129Sv background (Dent et al., 1997) were provided by A.L. Dent (Indiana University, Indianapolis, IN). All mice were maintained in a specific pathogen-free facility in accordance with University of Minnesota Institutional Animal Care and Use Committee and National Institutes of Health guidelines.

Antigen-specific B cell enrichment. The spleen and inguinal, axillary, brachial, cervical, mesenteric, and periaortic LN were harvested into PBS for each mouse analyzed. In experiments examining the proliferation and differentiation of PE-specific cells, tissues were minced in collagenase D (Roche) and EDTA (Sigma-Aldrich), as previously described (Vremec et al., 1992; Itano et al., 2003), to increase the number of antibody-secreting cells recovered.

A single-cell suspension was prepared and resuspended to 0.2 ml in Fc block, consisting of culture supernatant containing Fc receptor antibody 2.4G2 (American Type Culture Collection), 2% rat serum (Serotec), and 0.1% sodium azide (Sigma-Aldrich). Each sample was incubated with 1 µg PE (Prozyme) for 30 min on ice or 0.5 µg allophycocyanin for 30 min at room temperature. Incubation with antigen was followed by a wash in 15 ml of ice-cold sorter buffer (DPBS with 2% fetal bovine serum [Thermo Fisher Scientific] and 0.1% sodium azide). PE- or allophycocyanin-stained cells were then resuspended to a volume of 0.2 ml of sorter buffer, mixed with 25–50 µl anti-PE– or anti-allophycocyanin–conjugated magnetic microbeads (Miltenyi Biotec) and incubated for 30 min on ice, followed by one wash with 15 ml of sorter buffer. The cells were then resuspended in 3 ml of sorter buffer and passed over a magnetized LS column (Miltenyi Biotec). The column was washed twice with 3 ml of sorter buffer and then removed from the magnetic field. Bound cells were eluted by pushing 5 ml of sorter buffer through the column with a plunger.

Flow cytometry and cell counts. After centrifugation, cell pellets from the bound and flow through fractions were resuspended in 0.1 or 2 ml of sorter buffer, respectively, and 5 µl was removed from each sample for cell counting. The remaining cell suspensions were incubated with a cocktail of surface protein-specific antibodies for 25 min on ice and washed with sorter buffer. Antibodies used in various combinations were FITC-, AF647-, or Biotin-labeled GL7 (BD or eBioscience), AF700- or Pacific blue–labeled anti-CD38 (eBioscience or BioLegend), V500- or eF450-labeled anti-B220 (BD or eBioscience), AMCA-, PerCP-eF710–, or APC-labeled anti-IgM

(Jackson ImmunoResearch Laboratories, Inc or eBioscience), PerCP-Cy5.5– or eF450-labeled anti-IgD (BioLegend or eBioscience), FITC- or PerCP-Cy5.5–labeled anti-CD45.1 (eBioscience), and APC-eF780–labeled anti-CD11c, anti-Thy1.2, anti-F4/80, and anti-Gr-1 (eBioscience). Because the IgM-AMCA antibody cross reacts with rat IgM, samples were first stained with IgM-AMCA, washed, and then preincubated with purified rat IgM (eBioscience) before the addition of GL7. In some experiments, cells were then stained with eF605NC-conjugated streptavidin (eBioscience) for 15 min on ice and washed with sorter buffer.

For analysis of isotype switching, cells were pelleted after surface staining and resuspended with 1 ml of 2% formaldehyde for 20 min on ice, followed by a wash with 2 ml of PBS. The cells were pelleted and resuspended in 1 ml of 0.5% saponin and incubated for 1 h with a cocktail of biotin-labeled anti-IgG1 (A85-1), IgG2c (5.7), IgG2b (R12-3), IgG3(R40-82; all from BD), IgA (RMA-1), and IgE (RME-1) antibodies (both from BioLegend), followed by Pacific blue–labeled streptavidin (Invitrogen). In some cases, isotype-switched cells were gated as cells that did not bind anti-IgM or anti-IgD.

For Bcl-6 analysis, cells were fixed with 0.25 ml Foxp3 Fixative (eBioscience) for 25 min on ice. Samples were washed with 3 ml of sorter buffer and incubated with AF488-labeled anti–Bcl-6 AF488 (BD) for 1 h.

Flow cytometry was performed on a 4-laser (355, 405, 488, and 633 nm) or 5-laser (355, 405, 488, 561, and 640 nm) LSR II device (BD) and analyzed with FlowJo software (Tree Star). Cell sorting was performed by the University of Minnesota Flow Cytometry Core using a 3-laser (407, 488, and 633 nm) FACSAria (BD). Fluorescent AccuCheck counting beads (Invitrogen) were used to calculate total numbers of live lymphocytes in the column bound and flow through suspensions as previously described (Moon et al., 2009). Samples collected after PE and CFA injection often had a significant number of PE-labeled B cells that were not retained by the column. When this occurred, these cells were included in the total number of cells.

Injections. Mice were injected s.c. with 50 µl CFA (Sigma-Aldrich) emulsion containing 15 µg of R-PE (Prozyme) or 7.5 µg allophycocyanin (Prozyme) except where noted. For CD40:CD40L blockade, mice were injected intraperitoneally with 0.5–1 mg anti-CD40L (Mr-1; BioXcell) every other day for 3 d beginning on either day 5 or 17. For CD40 stimulation, mice were injected intraperitoneally with 250 µg anti-CD40 (FGK4.5; BioXcell) every other day for beginning on the day of PE and CFA injection.

Adoptive transfer experiments. Purified naive B cells were prepared from spleen and LN of CD45.1$^+$ mice using a B cell negative selection kit (Miltenyi Biotec). The B cells were washed in EHAA (Invitrogen), adjusted to a final concentration of 5×10^7 cells/ml in prewarmed EHAA, and incubated with 5 µM CFSE (Invitrogen) for 10 min at 37°C before they were injected intravenously into CD45.2 mice. Mice were injected with PE and CFA at least 1 d after adoptive transfer. Alternatively, cells were labeled with CellTrace violet (Invitrogen) according to the manufacturer's instructions. To control for mouse-to-mouse and experiment-to-experiment differences in the number of donor cells that could be detected in recipient animals, the frequency of donor B cells was normalized to 1% for each donor-derived PE-specific B cell population with the formula $c = (r/p) \times 1\%$, where p is the percentage of donor-derived PE-negative B cells obtained from the column flow through, r is the absolute number of PE-specific B cells obtained experimentally, and c is the absolute number after the correction.

Mixed bone marrow chimera experiments. Bone marrow cells were prepared by crushing bones from *Bcl6*$^{-/-}$ and 129Sv × B6.CD45.1 F_1 WT mice with a mortar and pestle in PBS. Bone marrow cells were labeled with anti-Thy1.2 and anti-NK1.1 (both from eBioscience), followed by incubation with rabbit complement (Cedarlane) for 30 min at 37°C to deplete T cells and NK cells. T cell– and NK cell–depleted *Bcl6*$^{-/-}$ and WT bone marrow cells were mixed 1:1 and 1–5 × 10^6 were injected into B6.CD45.1 recipient mice irradiated with 1,000 rad. The response of PE-specific cells in 129Sv × B6 CD45.1$^+$ F_1 mice was similar to that generated when control mixed chimeras were set up using *Bcl6*$^{+/-}$ or *Bcl6*$^{+/+}$ littermate controls (unpublished data). Injections were done 8–10 wk after bone marrow transplantation. Variations in the absolute numbers of PE-specific B cells as a result of slight differences in chimerism were corrected to 50% for each donor-derived PE-specific B cell population with the formula, $c = (r/p) \times 50\%$, where p is the percentage of donor-derived PE-negative B cells obtained from the column flow through, r is the absolute number of PE-specific B cells obtained experimentally, and c is the absolute number after the correction.

Immunofluorescence. LNs were harvested and frozen in OCT freezing medium (Sakura). 7-µm cryosections were dehydrated in acetone and blocked with 1% H_2O_2, culture supernatant containing 24G2 mAb plus 1% mouse and 1% rat serum, and avidin-biotin blocking reagents (Vector Laboratories). PE-binding cells were detected by incubating sections with PE followed by biotin-labeled anti-PE (produced by K. Pape), HRP-labeled streptavidin (PerkinElmer), and TSA-direct Cy3-tyramide (PerkinElmer). In some cases, the PE incubation was omitted as a negative control. GL7$^+$ cells were detected with FITC-labeled anti-GL7 (eBioscience), followed by AF488-labeled anti-FITC (Invitrogen). T cell areas were detected with biotin-labeled anti-Thy1.2 (eBioscience), followed by AMCA-labeled streptavidin (Jackson ImmunoResearch Laboratories, Inc.). B cell follicles were detected with AF647-labeled anti-IgD (eBioscience). Images were captured with 10, 20, and 40× objective lenses on an automated upright microscope (DM5500B; Leica) and a digital camera (DFC340FX; Leica). Photoshop (Adobe) was used to process the images for display.

Statistical analysis. All p-values were determined using an unpaired two-tailed Student's *t* test in Prism (GraphPad Software).

We thank J. Walter and R. Speier for expert technical assistance, D. Mueller and M. Pepper for reviewing the manuscript, T. Martin, P. Champoux, and N. Shah for flow cytometry assistance, and all members of the Jenkins Laboratory for helpful discussions.

This work was supported by grants from the National Institutes of Health (R01 AI036914 and R37 AI027998 to M.K. Jenkins, and T32 CA009138 and F32 AI091033 to J.J. Taylor).

The authors have no conflicting financial interests.

Submitted: 12 August 2011
Accepted: 30 January 2012

REFERENCES

Anderson, S.M., M.M. Tomayko, A. Ahuja, A.M. Haberman, and M.J. Shlomchik. 2007. New markers for murine memory B cells that define mutated and unmutated subsets. *J. Exp. Med.* 204:2103–2114. http://dx.doi.org/10.1084/jem.20062571

Benson, M.J., R. Elgueta, W. Schpero, M. Molloy, W. Zhang, E. Usherwood, and R.J. Noelle. 2009. Distinction of the memory B cell response to cognate antigen versus bystander inflammatory signals. *J. Exp. Med.* 206: 2013–2025. http://dx.doi.org/10.1084/jem.20090667

Blink, E.J., A. Light, A. Kallies, S.L. Nutt, P.D. Hodgkin, and D.M. Tarlinton. 2005. Early appearance of germinal center–derived memory B cells and plasma cells in blood after primary immunization. *J. Exp. Med.* 201:545–554. http://dx.doi.org/10.1084/jem.20042060

Chan, T.D., D. Gatto, K. Wood, T. Camidge, A. Basten, and R. Brink. 2009. Antigen affinity controls rapid T-dependent antibody production by driving the expansion rather than the differentiation or extrafollicular migration of early plasmablasts. *J. Immunol.* 183:3139–3149. http://dx.doi.org/10.4049/jimmunol.0901690

Coffey, F., B. Alabyev, and T. Manser. 2009. Initial clonal expansion of germinal center B cells takes place at the perimeter of follicles. *Immunity.* 30:599–609. http://dx.doi.org/10.1016/j.immuni.2009.01.011

Dent, A.L., A.L. Shaffer, X. Yu, D. Allman, and L.M. Staudt. 1997. Control of inflammation, cytokine expression, and germinal center formation by BCL-6. *Science.* 276:589–592. http://dx.doi.org/10.1126/science.276.5312.589

Dogan, I., B. Bertocci, V. Vilmont, F. Delbos, J. Mégret, S. Storck, C.A. Reynaud, and J.C. Weill. 2009. Multiple layers of B cell memory with

different effector functions. *Nat. Immunol.* 10:1292–1299. http://dx.doi.org/10.1038/ni.1814

Erickson, L.D., B.G. Durell, L.A. Vogel, B.P. O'Connor, M. Cascalho, T. Yasui, H. Kikutani, and R.J. Noelle. 2002. Short-circuiting long-lived humoral immunity by the heightened engagement of CD40. *J. Clin. Invest.* 109:613–620.

Fecteau, J.F., G. Côté, and S. Néron. 2006. A new memory CD27-IgG+ B cell population in peripheral blood expressing VH genes with low frequency of somatic mutation. *J. Immunol.* 177:3728–3736.

Fukuda, T., T. Yoshida, S. Okada, M. Hatano, T. Miki, K. Ishibashi, S. Okabe, H. Koseki, S. Hirosawa, M. Taniguchi, et al. 1997. Disruption of the Bcl6 gene results in an impaired germinal center formation. *J. Exp. Med.* 186:439–448. http://dx.doi.org/10.1084/jem.186.3.439

Garside, P., E. Ingulli, R.R. Merica, J.G. Johnson, R.J. Noelle, and M.K. Jenkins. 1998. Visualization of specific B and T lymphocyte interactions in the lymph node. *Science.* 281:96–99. http://dx.doi.org/10.1126/science.281.5373.96

Han, S., K. Hathcock, B. Zheng, T.B. Kepler, R. Hodes, and G. Kelsoe. 1995. Cellular interaction in germinal centers. Roles of CD40 ligand and B7-2 in established germinal centers. *J. Immunol.* 155:556–567.

Itano, A.A., S.J. McSorley, R.L. Reinhardt, B.D. Ehst, E. Ingulli, A.Y. Rudensky, and M.K. Jenkins. 2003. Distinct dendritic cell populations sequentially present antigen to CD4 T cells and stimulate different aspects of cell-mediated immunity. *Immunity.* 19:47–57. http://dx.doi.org/10.1016/S1074-7613(03)00175-4

Jung, J., J. Choe, L. Li, and Y.S. Choi. 2000. Regulation of CD27 expression in the course of germinal center B cell differentiation: the pivotal role of IL-10. *Eur. J. Immunol.* 30:2437–2443. http://dx.doi.org/10.1002/1521-4141(2000)30:8<2437::AID-IMMU2437>3.0.CO;2-M

Klein, U., R. Küppers, and K. Rajewsky. 1997. Evidence for a large compartment of IgM-expressing memory B cells in humans. *Blood.* 89:1288–1298.

Klein, U., K. Rajewsky, and R. Küppers. 1998. Human immunoglobulin (Ig)M^+IgD^+ peripheral blood B cells expressing the CD27 cell surface antigen carry somatically mutated variable region genes: CD27 as a general marker for somatically mutated (memory) B cells. *J. Exp. Med.* 188:1679–1689. http://dx.doi.org/10.1084/jem.188.9.1679

MacLennan, I.C.M. 1994. Germinal centers. *Annu. Rev. Immunol.* 12:117–139. http://dx.doi.org/10.1146/annurev.iy.12.040194.001001

Manz, R.A., M. Löhning, G. Cassese, A. Thiel, and A. Radbruch. 1998. Survival of long-lived plasma cells is independent of antigen. *Int. Immunol.* 10:1703–1711. http://dx.doi.org/10.1093/intimm/10.11.1703

Maul, R.W., and P.J. Gearhart. 2010. AID and somatic hypermutation. *Adv. Immunol.* 105:159–191. http://dx.doi.org/10.1016/S0065-2776(10)05006-6

McHeyzer-Williams, L.J., and M.G. McHeyzer-Williams. 2005. Antigen-specific memory B cell development. *Annu. Rev. Immunol.* 23:487–513. http://dx.doi.org/10.1146/annurev.immunol.23.021704.115732

Moon, J.J., H.H. Chu, J. Hataye, A.J. Pagán, M. Pepper, J.B. McLachlan, T. Zell, and M.K. Jenkins. 2009. Tracking epitope-specific T cells. *Nat. Protoc.* 4:565–581. http://dx.doi.org/10.1038/nprot.2009.9

Nurieva, R.I., Y. Chung, G.J. Martinez, X.O. Yang, S. Tanaka, T.D. Matskevitch, Y.H. Wang, and C. Dong. 2009. Bcl6 mediates the development of T follicular helper cells. *Science.* 325:1001–1005. http://dx.doi.org/10.1126/science.1176676

Pape, K.A., J.J. Taylor, R.W. Maul, P.J. Gearhart, and M.K. Jenkins. 2011. Different B cell populations mediate early and late memory during an endogenous immune response. *Science.* 331:1203–1207. http://dx.doi.org/10.1126/science.1201730

Schittek, B., and K. Rajewsky. 1992. Natural occurrence and origin of somatically mutated memory B cells in mice. *J. Exp. Med.* 176:427–438. http://dx.doi.org/10.1084/jem.176.2.427

Schwickert, T.A., G.D. Victora, D.R. Fooksman, A.O. Kamphorst, M.R. Mugnier, A.D. Gitlin, M.L. Dustin, and M.C. Nussenzweig. 2011. A dynamic T cell-limited checkpoint regulates affinity-dependent B cell entry into the germinal center. *J. Exp. Med.* 208:1243–1252. http://dx.doi.org/10.1084/jem.20102477

Seifert, M., and R. Küppers. 2009. Molecular footprints of a germinal center derivation of human $IgM^+(IgD^+)CD27^+$ B cells and the dynamics of memory B cell generation. *J. Exp. Med.* 206:2659–2669. http://dx.doi.org/10.1084/jem.20091087

Shinall, S.M., M. Gonzalez-Fernandez, R.J. Noelle, and T.J. Waldschmidt. 2000. Identification of murine germinal center B cell subsets defined by the expression of surface isotypes and differentiation antigens. *J. Immunol.* 164:5729–5738.

Tarlinton, D.M. 2008. Evolution in miniature: selection, survival and distribution of antigen reactive cells in the germinal centre. *Immunol. Cell Biol.* 86:133–138. http://dx.doi.org/10.1038/sj.icb.7100148

Tomayko, M.M., N.C. Steinel, S.M. Anderson, and M.J. Shlomchik. 2010. Cutting edge: Hierarchy of maturity of murine memory B cell subsets. *J. Immunol.* 185:7146–7150. http://dx.doi.org/10.4049/jimmunol.1002163

Toyama, H., S. Okada, M. Hatano, Y. Takahashi, N. Takeda, H. Ichii, T. Takemori, Y. Kuroda, and T. Tokuhisa. 2002. Memory B cells without somatic hypermutation are generated from Bcl6-deficient B cells. *Immunity.* 17:329–339. http://dx.doi.org/10.1016/S1074-7613(02)00387-4

Vremec, D., M. Zorbas, R. Scollay, D.J. Saunders, C.F. Ardavin, L. Wu, and K. Shortman. 1992. The surface phenotype of dendritic cells purified from mouse thymus and spleen: investigation of the CD8 expression by a subpopulation of dendritic cells. *J. Exp. Med.* 176:47–58. http://dx.doi.org/10.1084/jem.176.1.47